Human Molecular Genetics, 1997, Vol. 6, No. 8 **1225–1231**

Characterization of unconventional *MYO6*, the human homologue of the gene responsible for deafness in Snell's waltzer mice

Karen B. Avraham[1,*], Tama Hasson[2], Tama Sobe[1], Binaifer Balsara[3], Joseph R. Testa[3], Anne B. Skvorak[4], Cynthia C. Morton[4,5], Neal G. Copeland[6] and Nancy A. Jenkins[6]

[1]Department of Human Genetics, Sackler School of Medicine, Tel Aviv University, Tel Aviv 69978, Israel, [2]Departments of Biology and Pathology, Yale University, New Haven, CT 06511, USA, [3]Department of Medical Oncology, Fox Chase Cancer Center, Philadelphia, PA 19111, USA, [4]Department of Pathology and [5]Department of Obstetrics, Gynecology and Reproductive Biology, Brigham and Women's Hospital and Harvard Medical School, Boston, MA 02115, USA and [6]Mammalian Genetics Laboratory, ABL-Basic Research Program, NCI-Frederick Cancer Research and Development Center, Frederick, MD 21702, USA

Received February 25, 1997; Revised and Accepted May 8, 1997

DDBJ/EMBL/GenBank accession no. U90236

Deafness is the most common form of sensory impairment in humans. Mutations in unconventional myosins have been found to cause deafness in humans and mice. The mouse recessive deafness mutation, Snell's waltzer, contains an intragenic deletion in an unconventional myosin, myosin VI (locus designation, *Myo6*). The requirement for *Myo6* for proper hearing in mice makes this gene an excellent candidate for a human deafness disorder. Here we report the cloning and characterization of the human unconventional myosin VI (locus designation, *MYO6*) cDNA. The *MYO6* gene maps to human chromosome 6q13. The isolation of the human gene makes it now possible to determine if mutations in *MYO6* contribute to the pathogenesis of deafness in the human population.

INTRODUCTION

Deafness is the most common form of sensory impairment in humans. Approximately 1 out of 1000 individuals is born deaf, while about 1 out of 10 individuals become deaf or hard of hearing during their lifetime (1). Hearing impairment can result from a variety of injuries or diseases, and occurs both in association with other symptoms, or as an isolated finding. Hearing loss can be genetic or acquired, and occurs both prelingually due to genetic defects or childhood diseases, or postlingually due to inherited gene mutations, environmental noise pollution, infection or presbycusis. Despite its prevalence in the human population, very little is known about the molecular events leading to deafness and about the genes that control normal hearing. The study of genes involved in hearing will provide us with clues regarding the molecular basis of hearing transduction.

As many as 100 genes may be involved in non-syndromic deafness with an autosomal recessive mode of inheritance (2). It has been very difficult to identify these genes because of the absence of characteristic clinical signs in deaf individuals, genetic heterogeneity of deafness, and small family populations. To date, only 13 autosomal recessive deafness loci have been described (3). Additional genes for autosomal deafness exist, but the lack of suitable families for linkage analysis makes discovering these genes difficult. Therefore, genes responsible for hearing loss in the mouse provide another method to identify potential human deafness loci. The structure and development of the inner ear, and the pathology leading to hearing impairment is very similar between mice and humans (4).

Over 60 mouse mutations affecting the inner ear have been mapped in the mouse genome (5). Two of the most recently identified mouse deafness genes are unconventional myosins, demonstrating the important role in hearing of this family of proteins (6,7). Unconventional myosins are molecular motors defined by their conserved head or motor domain, light-chain binding neck or regulatory domain, and a unique tail domain. Upon interacting with actin, they convert energy from ATP hydrolysis to mechanical force and have been found to play a role in sensory hair cells, melanocytes, retinal epithelia and neurons (8,9). Myosins are crucial for the proper function of the hair cells, the sensory cells of the inner ear, since mutations in two of these proteins cause deafness in mice, and in one case, in humans. The mouse unconventional *Myo6* was discovered during a positional cloning approach to clone the gene responsible for deafness in the Snell's waltzer (*sv*) mutation (6). Myosin VIIA was found to be defective in shaker-1 (*sh1*) mice, an autosomal recessive mutation characterized by deafness and vestibular dysfunction and in human Usher syndrome type 1B, an inherited disease characterized by deafness, vestibular dysfunction and retinitis pigmentosa (7,10). The involvement of myosin VIIA in both human and mouse deafness, the similarity of the human and mouse auditory systems, and the existence of additional unidentified human deafness loci suggest that *Myo6* will also be involved in human deafness. Here

*To whom correspondence should be addressed. Tel: +972 3 640 7030; Fax: +972 3 640 9900; Email: karena@post.tau.ac.il

we report the cloning and characterization of the human *MYO6* cDNA, which maps to human chromosome 6q13. Cloning the human homologue of the mouse gene provides a method for discovering an additional human deafness locus, circumventing the need for conventional linkage analysis. The requirement for *Myo6* in hearing in mice makes this gene an excellent candidate for a human deafness disorder.

RESULTS

The human *MYO6* coding sequence

The human homologue of the Snell's waltzer locus, *MYO6*, was isolated by screening a human cerebral cDNA library with the mouse *Myo6* cDNA (6). Four clones, HVI-13 (from nucleotides –120 to 1045), HVI-11 (nt 1955–2917), HVI-16 (nt 2394–3079) and HVI-18 (nt 2977 to end), were isolated and sequenced (Fig. 1a). Comparison of the sequence of HVI-13 with that of the mouse cDNA indicated that this clone was homologous to the 5′ end of mouse *Myo6*. HVI-13 contained 120 bp of the 5′ untranslated region (UTR) preceding the same ATG start site identified in the mouse. The remaining clones were derived from the central and 3′ end of the cDNA, including 208 bp from the 3′ UTR (HVI-18). The poly(A^+) tail was not recovered during the screening. Alignment of the human cDNA clones to the full-length cDNA sequence revealed a gap of ~1000 nt (between HVI-13 and HVI-11). RT-PCR was performed on human cerebral RNA using primers derived from the human cDNA clones on either side of the gap. The sequences of the cDNA clones and RT-PCR products were assembled and revealed a predicted open reading frame (ORF) of 3789 bp (Fig. 1a and b). cDNA nucleotide position +1 was assigned to the first nucleotide of the start codon (ATG). The human *MYO6* cDNA is predicted to encode a protein of 1263 amino acids with a relative molecular weight of 142 kDa (Fig. 1b). The protein contains a head/motor region of 776 amino acids, containing an ATP-binding domain (GESGAGKT, amino acids 151–158) and actin-binding sequences (11,12). The motor domain contains a conserved threonine residue at amino acid 405, which may serve as a site for phosphorylation (Figs 1b and 2a). Following the motor domain is a 52 amino acid region that is unique to myosin VI, whereas in other unconventional myosins, the light chain binding site immediately follows the motor region. The light chain binding site that follows is a single IQ motif, serving as a site for calmodulin (RAEACIKMQKTIRMWLCKRR, amino acids 829–848) (11). The tail, like that of the mouse myosin VI, contains a region predicted to be a coiled-coil of 192 amino acids (13), followed by a distal globular region of 232 amino acids (Fig. 1b).

Comparison of human MYOSIN VI with other myosin VI species

Myosin VI was first isolated in *Drosophila* in the process of isolating novel actin-binding proteins from embryonic extracts

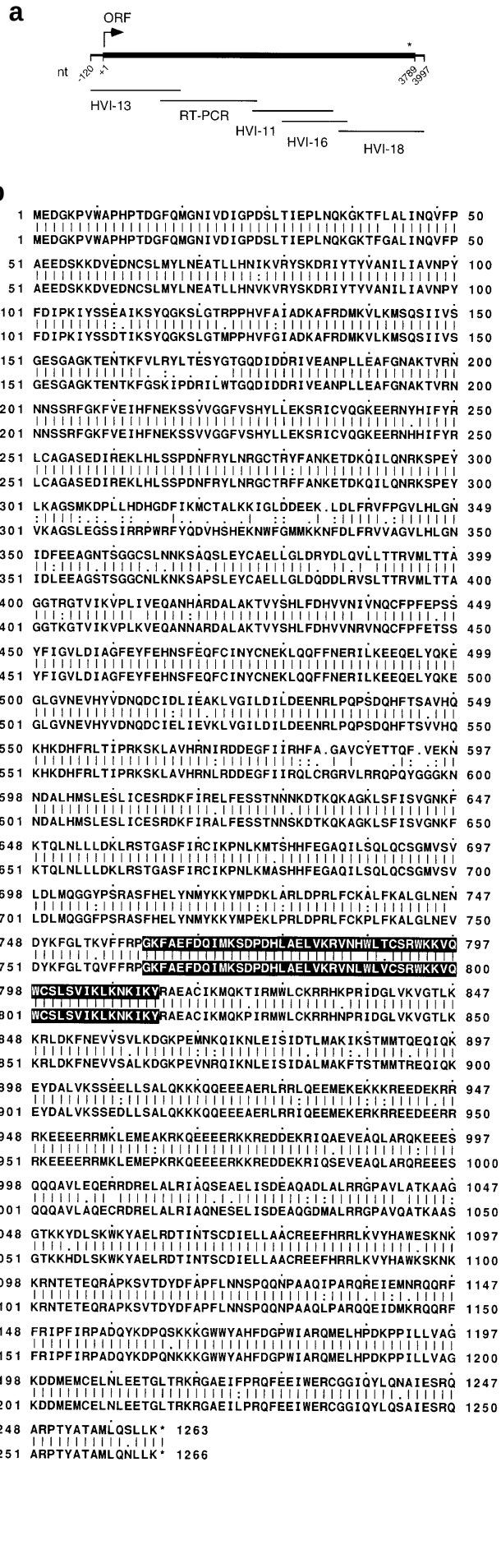

Figure 1. Human *MYO6* cDNA and amino acid sequence. (**a**) Schematic representation of overlapping cDNA clones and RT-PCR generated fragment used to construct full length *MYO6* cDNA. Shaded box represents the open reading frame; asterisk marks stop codon (TAG); nt = nucleotide number. (**b**) Amino acid comparison of human (top) and mouse (bottom) myosin VI predicted amino acid sequence. The ~50 amino acid region unique to myosin VI is shaded. The nucleotide sequence has been submitted to GenBank (accession no. U90236). Amino acid sequences were compared using the Bestfit program from the Wisconsin GCG package (33).

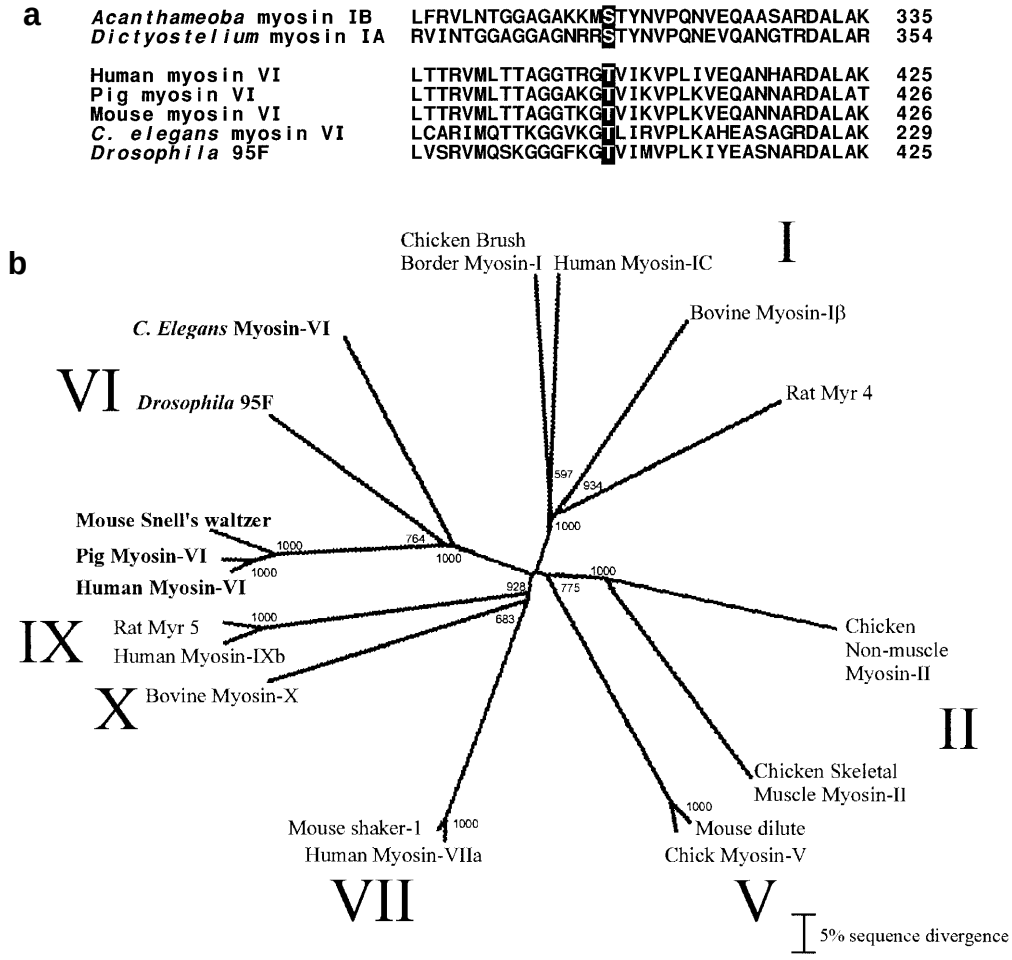

Figure 2. Comparison of myosin VI species. (**a**) Alignment over the phosphorylation site from different myosin VI species. The conserved site is shaded. Amino acid sequences were compared using the Bestfit program from the Wisconsin GCG package (33). (**b**) An unrooted phylogenetic tree of myosins-VI and other vertebrate myosins based on the amino acid sequence of their head domains. This phylogenetic tree was produced using the default parameters of the CLUSTAL W program. The lengths of the branches connecting two sequences are proportional to the percent amino acid sequence divergence between the two sequences. The number of times two sequences or groups of sequences were joined together out of 1000 trials is indicated as a bootstrapping value next to the node. Low bootstrapping values indicate uncertainty about the placement of a given branch. Myosin VI proteins are shown in bold. Accession numbers: human myosin VI (U90236); pig myosin VI (Z35331); mouse *sv* (U49739); *Drosophila* 95F (X67077); *C.elegans* myosin VI (U52517); chicken brush border myosin-I (X58479); human myosin-IC (U14391); bovine myosin-Iβ (Z22852); rat Myr4 (X71997); chicken non-muscle myosin-IIA (SP P14105); chicken skeletal muscle myosin-II (SP P13538); mouse dilute (X57377); chick myosin-V (Z11718); mouse *sh1* (U81453); human myosin-VIIA (U34227); bovine myosin-X (U55042); rat Myr 5 (X77609); human myosin-IXB (M85411). All above sequences are from GenBank unless indicated as SwissProt (SP).

(14). This molecule was subsequently found to play an important role in the organization of the syncytial blastoderm and transportation of cytoplasmic particles (15,16). The pig myosin VI was isolated during a characterization of myosin isoforms expressed in kidney proximal tubule cells (11). Recently, a partial sequence of nematode myosin VI was isolated as well (J.P.Baker and M.A.Titus, personal communication). Comparison of the cDNA and predicted amino acid sequences from *Drosophila*, *Caenorhabditis elegans*, pig, mouse and human myosin VI shows strong evolutionary conservation not only in the head or motor domain, but also in the distal tail region (Table 1; Fig. 2a), whose structure and binding interactions may determine subcellular localization and function (9). The threonine site at amino acid 405 in human myosin VI is conserved between all myosin VI species examined (Fig. 2a).

Table 1. Amino acid identity between myosin VI species

	Percent identity to human myosin VI protein		
	Motor domain	Distal tail	Entire ORF
Pig	95.1	94.6	94.8
Mouse	88.6	94.4	90.2
Drosophila	55.8	61.2	52.3
C.elegans	NA	NA	46.4

NA, not available due to partial sequence.

Phylogenetic sequence comparisons of the conserved head domains of unconventional myosins have been used to demonstrate that the myosins are grouped into several distinct classes

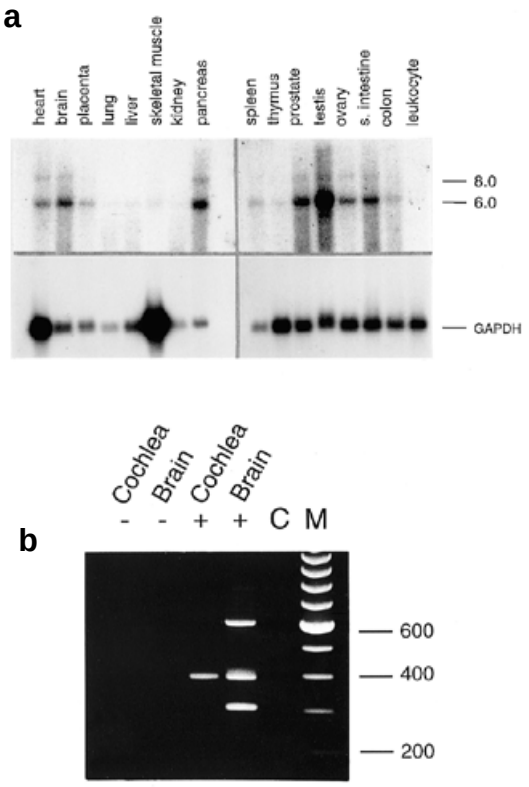

Figure 3. *MYO6* expression in human tissues. (**a**) Northern blot analysis of 2 μg of poly(A)$^+$ RNA derived from human tissues. Blots were probed with a portion of the human *MYO6* cDNA. The same filters were stripped and rehybridized with a GAPDH cDNA probe to control for RNA loading. *MYO6* transcript sizes, in kb, are shown to the right. (**b**) RT-PCR analysis of RNA samples from human fetal cochlea and brain. (+) denotes RT+ samples, (–) denotes RT– controls. C = PCR control with no DNA template. The PCR reaction was run on a 1% agarose gel with 100 bp markers (M) (Gibco/BRL).

(9). An unrooted phylogenetic tree of myosins VI and other vertebrate myosins based on the amino acid sequence of their head domains is shown in Figure 2b. Included for the first time in this analysis is the sequence of the human and *C.elegans* myosin VI.

Expression and localization of myosin VI

The expression of human *MYO6* was examined in both fetal and adult human tissues. The human *MYO6* cDNA clone HVI-18, containing a portion of the tail region, was hybridized to northern blots containing RNA from a series of adult human tissues (Fig. 3a). The major *MYO6* transcript is ~6.0 kb and was observed in most tissues examined. A less abundant 8.0 kb transcript was also detected (Fig. 3a) The two transcripts were also observed in the mouse (6). Highest levels of expression of *MYO6* in human tissues were seen in brain, pancreas, prostate, testis and small intestine.

Expression of *MYO6* was observed in human fetal cochlea and brain by RT-PCR analysis, using PCR primers from the tail portion of the ORF (Fig. 3b). The expected product of 391 bp was detected in both fetal cochlea and brain. In the fetal brain, two additional products of ~300 and 600 bp were detected. These products may represent alternate splice forms required only during brain development, since RT-PCR using the same primers on human adult brain produced only the 391 bp product (data not shown).

An immunofluorescence study very clearly shows the expression of myosin VI in the cuticular plate of the hair cell, the portion of the cell supporting the stereocilia, in cochlea of 3 week old mice. Affinity purified rabbit anti-myosin VI-tail antibodies (11) were incubated with whole mount wild-type mouse cochlea and visualized with a fluorescein-conjugated secondary antibody. To visualize the actin-rich domains within the organ of Corti, the cochlea was also stained with rhodamine-conjugated phalloidin. Myosin VI was concentrated within the inner and outer hair cells of the sensory epithelium, and in particular, in the cuticular plate (double arrows, Fig. 4), but not along the length of the stereocilia (arrow, Fig. 4) of the hair cells.

Human chromosomal localization of *MYO6*

The human chromosomal location of *MYO6* was determined by fluorescence *in situ* hybridization (FISH) analysis. Hybridization of the HVI-13 probe to metaphase spreads revealed specific labeling on human chromosome 6. Fluorescent signals were detected on chromosome 6 in 21 of 35 metaphase spreads. Among a total of 93 signals observed, 33 (35.4%) were located on 6q. The vast majority (29 of 33) of signals on chromosome 6 were located at band 6q13 (Fig. 5a). Specific signals on 6q were distributed as follows: one chromatid (11 cells), two chromatids (9 cells), three chromatids (0 cells), four chromatids (1 cell).

A search in the Genome Database (GDB, The Johns Hopkins University, Baltimore, MD) revealed three microsatellite markers that have been mapped onto 6q13 (Fig. 5b). These markers, *D6S280*, *D6S254* and *D6S313*, may be used for linkage analysis (17). Should one of these markers and a deafness locus co-segregate, *MYO6* becomes a candidate for a human deafness locus, facilitating analysis of the molecular basis for the mutation.

DISCUSSION

We have cloned and characterized the human cDNA homologous to the mouse unconventional *Myo6*, a gene crucial for sensorineural hearing in the mouse (6). The structure and function of the mouse and human inner ear is remarkably similar, and thus the mouse has proved to be an invaluable model for studying human hearing loss. The first genes responsible for autosomal recessive deafness were initially identified in the mouse (6,7), demonstrating the value of the mouse for identifying and studying human deafness genes. The isolation of the mouse unconventional *Myo6* gene has been instrumental in cloning the human *MYO6* gene, and facilitates the discovery of mutations in the human deaf population.

The function and regulation of myosin VI remains largely unknown, although homology of a potentially phosphorylated amino acid between all myosins-VI and myosins-I of *Acanthamoeba* suggests a similar form of regulation (9). Actin-activated Mg-ATPase and motility of *Acanthamoeba* myosins-I require phosphorylation of a serine or threonine residue by a heavy-chain kinase (18). No other vertebrate myosins of any class share this site, except for myosins-VI. The conservation of this residue in this class of myosins has led to the postulation that myosin VI requires heavy chain phosphorylation for enzymatic and mechanochemical activity (19).

Gene-tree phylogenetic analyses are crucial to determine the evolutionary relatedness or homology between proteins (20).

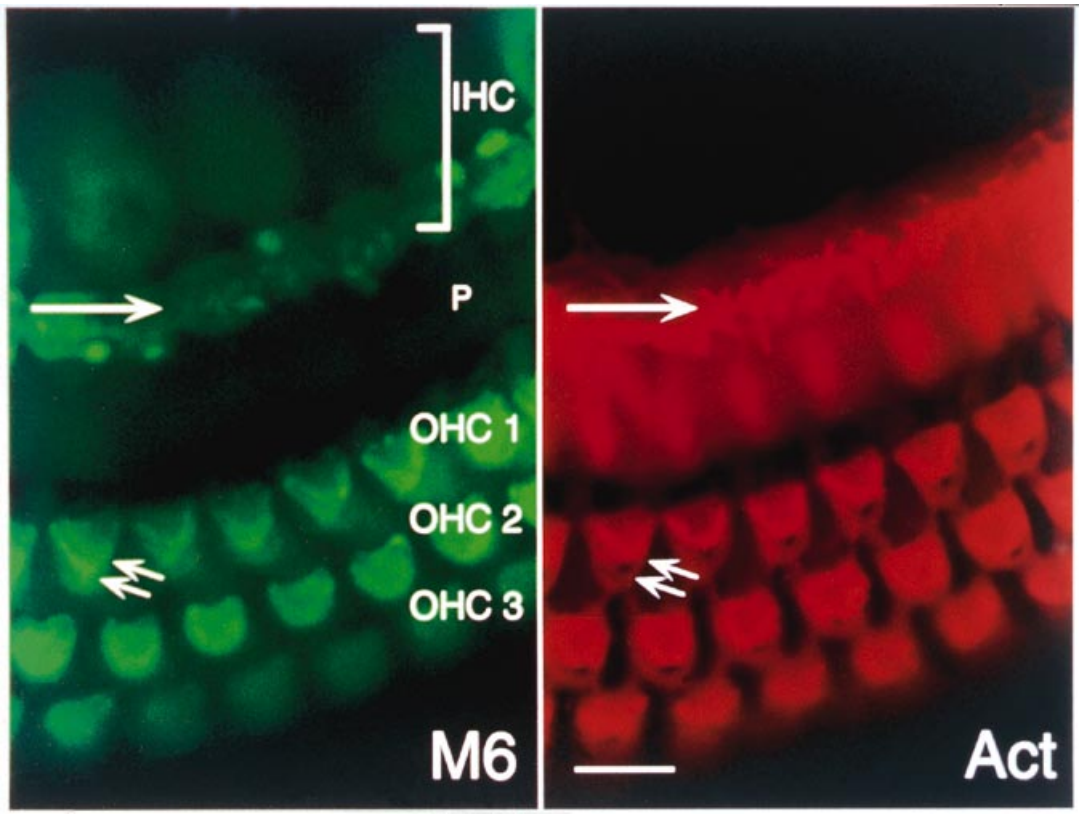

Figure 4. Localization of myosin VI and F-actin in the apical domain of 3 week old wild-type mouse cochleas by immunohistochemistry. An immunofluorescence micrograph of an optical section through the organ of Corti perpendicular to the cochlear axis is shown. The sample was stained with affinity purified rabbit anti-myosin VI-tail antibodies (M6; green) and the F-actin binding compound rhodamine-conjugated phalloidin (Act; red). The locations of the inner hair cells (IHC) and three outer hair cell (OHC) rows are marked. The stereocilia are clearly visible as V-shaped staining bundles in the outer hair cells and as a row of brightly staining material in the inner hair cells. At this high magnification, it is clear that the inner hair cell stereocilia (marked with a long arrow) do not stain brightly for myosin VI, while the protein is present in the cuticular plate at the base of the stereocilia (double arrows) in outer hair cell rows. Non-immune controls indicated that the staining pattern at the stereocilia bases was not due to bleed-through from the rhodamine-phalloidin signal. The lack of bleed-through into the fluorescein channel is also evident by the absence of signal from cells (e.g., pillar cells) which are F-actin rich, but do not contain myosin VI. Myosin VI is not expressed in the actin-rich pillar cells (P). Scale bar = 10 μm.

Protein sequence comparison between different myosin VI species shows a remarkably high degree of conservation, considering the diversity of the organisms, suggesting they retain a similar and vital function. From studies done in *Drosophila*, we can predict that myosin VI has an important role in development, and from work in the mouse, that myosin VI is crucial for proper hearing.

The expression of *MYO6* in human fetal cochlea demonstrates the importance of myosin VI in the mammalian inner ear and supports its potential role in human inner ear pathology. Within the hair cells, myosin VI is enriched in the cuticular plate, an actin-rich structure at the base of the stereocilia. To carry out mechanical transduction, the hair cell utilizes an actin-rich hair bundle made up of the stereocilia, which is inserted rigidly into the cuticular plate. The arrangement and number of stereocilia at the surface of the hair cell is very precise and is formed in a series of steps to generate the complex actin cytoskeleton (21). Therefore, proper hair bundle formation is crucial for hearing. Myosin VI may play an important role in this formation due to its high level of expression in the cuticular plate. Other unconventional myosins are also expressed in the hair cells, namely myosin-Iβ and myosin VIIa (locus designation, *MYO7A*) (22,23). Genetic analysis of *MYO6* and *MYO7A* reveals differences in the role of these motors in the sensory hair cell, since mutations in both cause deafness in mice (6,7). Myosin-Iβ is located at the stereociliary tips (22), whereas myosin VIIa is not located at the tips, but distributed along the length of the stereocilia (23). The different localization in the hair cell of these three unconventional myosins suggests that they have different functions in the sensory hair cell.

Comparative genome mapping between human and mouse has revealed very high conservation of linkage organization between the two organisms (24). Approximately 140–180 conserved chromosomal segments of linked homologous genes have been identified between the human and mouse genome maps (25). The mouse *Myo6* gene maps to the central region of chromosome 9, in a region homologous to human chromosomes 6 and 15 (26). In the mouse, *Myo6* maps between *Gsta* and *Htr1b*; the human homologues, *GSTA2* and *HTR1B*, both map to human chromosome 6 (27,28).

Two loci for non-syndromic autosomal dominant deafness have been localized to human chromosome 6, one at 6q22–q23 (DFNA10) (29) and the second at 6q21 (DFNA13; R.Smith, personal communication), though no recessive loci have been identified on this chromosome to date. Microsatellite markers localized to 6q13 can be used to identify linkage in potential deaf

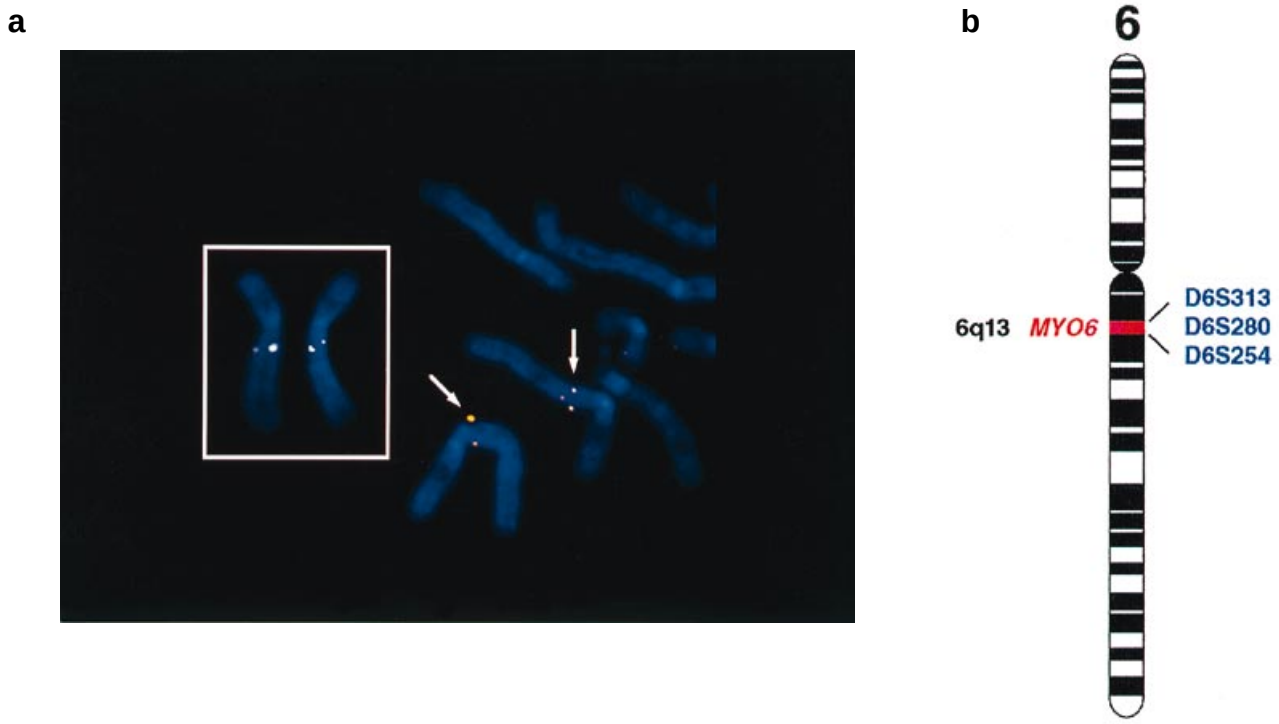

Figure 5. Human chromosomal localization of *MYO6*. (**a**) Chromosomal mapping of the *MYO6* gene to human chromosomes by FISH. Figure depicts a partial metaphase spread showing hybridization of fluorescein-labeled HVI-13 probe to 6q13 (arrows). Inset: Hybridization to chromosome 6 from other metaphase spreads. The composite photographs represent computer-enhanced, merged images of fluorescein signals and DAPI stained chromosomes. (**b**) Ideogram of chromosome 6 showing the location of *MYO6*. Microsatellite markers mapped to 6q13 are shown to the right.

individuals. Mutations in *MYO6* can then be identified by sequencing the *MYO6* coding region and/or by hybridizing RNA from normal and deaf individuals. Discovering mutations in *MYO6* in the human deaf population may ultimately lead to better diagnosis of inherited deafness and help improve the quality of life of deaf individuals by suggesting new means of treating or preventing hearing loss.

MATERIALS AND METHODS

Isolation of cDNA clones

An oligo(dT) and random primed human cerebral brain cDNA library in a λgt10 vector (Clontech) was screened with the mouse *Myo6* cDNA (6). 10^6 p.f.u. were plated at a density of 5×10^4 p.f.u./15 cm plate and replica filters were hybridized with [α-^{32}P]dCTP using a random priming labeling kit (Amersham). λ DNA was isolated using a Qiagen DNA preparation kit.

RT-PCR

Poly(A)$^+$ RNA, isolated from human brain (Clontech), was reverse-transcribed using oligo(dT) and random hexanucleotide primers (Invitrogen) and SuperScript II reverse transcriptase (Gibco BRL). PCR primers 23617 (5′-gct gca cta gat act ttg cta ac-3′; nt 878–901) and 22779 (5′-gtg gtg gct tgt cat ctt taa g-3′; nt 2064–2085) were denatured at 94°C for 1 min, annealed at 60°C for 1 min, and extended at 72°C for 1 min for 30 cycles.

Sequence analysis

Sequencing of plasmid DNA was done using the PRISM™ Ready Reaction DyeDeoxy™ Terminator Cycle Sequencing Kit (Perkin Elmer). RT-PCR products were purified on columns to remove primers (Centricep columns, Princeton Separations). *Taq*-based cycle sequencing reactions were done using fluorescent dideoxy terminators. Reactions were read on an ABI Model 373A DNA Sequencer (Applied Biosystems).

Expression analysis by northern blot and RT-PCR

Northern blots containing 2 μg of poly(A)$^+$ RNA from 16 different human tissues were hybridized with a portion of the human *MYO6* cDNA (Multiple Tissue Northern I and II, Clontech) according to the manufacturer's protocol. The probe was a PCR-generated fragment of the tail (nt 2799–3677) derived from cDNA clone HVI-18. Uniformity of loading was checked by hybridization to a chicken glycerol-3-aldehyde phosphate dehydrogenase (GAPDH) probe.

Total RNA from human fetal cochlea and brain was extracted using the guanidine isothiocyanate method (30). Total RNA (2.5 μg) was reverse transcribed using the SuperScript II kit of Gibco/BRL. Parallel reactions without reverse transcriptase were performed to control for DNA contamination of RNA samples. Ten percent of the reverse transcriptase (± RT) reaction was used as template for PCR. PCR reagents including *Taq* polymerase were from Perkin Elmer and were used according to the manufacturer's instructions. PCR primers 211253 (5′-ggatctgt-gttcaaggcaaag-3′; mouse cDNA nt 1073–1092; corresponding to

human cDNA nt 701–721) and 202592 (5′-cagattgcagccacct-gaag-3′; nt 1073–1092) were denatured at 94°C for 45 s, annealed at 58°C for 45 s, and extended at 72°C for 1 min for 30 cycles.

Immunohistochemistry

The mice cochlea were treated as described previously (6). Briefly, the dissected cochlea from 3 week old wild-type mice were fixed then treated with affinity purified rabbit anti-myosin VI-tail or control non-immune rabbit IgG. Samples were incubated with fluorescein-conjugated anti-rabbit secondary antibody (Cappel) and rhodamine-conjugated phalloidin (Molecular Probes), before being placed in PBS-glycerol mounting media (Citifluor). Samples were observed using a BioRad MRC600 laser scanning confocal microscope, captured using the COMOS program, and contrast enhanced in Photoshop 3.0 before compilation into a two-panelled figure in Canvas 3.52.

FISH analysis

Metaphase spreads from normal human female lymphocytes were prepared as described (31). The *MYO6* cDNA clone, HVI-13 (from nt –120 to 1045), was labeled with biotin-16-dUTP by nick translation. FISH and detection of immunofluorescence were performed as previously described (32). The chromosome preparations were stained with diamidino-2-phenylindole (DAPI) and observed with a Zeiss Axiophot fluorescence microscope. Images were captured with a cooled CCD camera connected to a Power Macintosh 8500 work station. Digitized images of DAPI staining and fluorescent signals were merged using Oncor Image software.

ABBREVIATIONS

bp, base pair; FISH, fluorescence *in situ* hybridization; kb, kilobase pair; kDa, kilodalton; ORF, open reading frame; PCR, polymerase chain reaction; p.f.u., plaque forming units; RT-PCR, reverse transcription-polymerase chain reaction; UTR, untranslated region.

ACKNOWLEDGEMENTS

Research sponsored in part by the National Cancer Institute, DHHS, with ABL; by NIH grant CA-06927 and an appropriation from the Commonwealth of Pennsylvania to B.B. and J.R.T.; by NIH grant DK38979 and a grant from the Deafness Research Foundation to T.H.; by NIH grant DC00038-05 to A.B.S. and NIH grant DC00871 to C.C.M.; and by Tel Aviv University.

REFERENCES

1. Nadol, J.B. (1993) *N. Engl. J. Med.* **329**, 1092–1102.
2. Morton, N.E. (1991) *Ann. NY Acad. Sci.* **630**, 16–31.
3. Van Camp, G. and Smith, R.J.H. (April, 1997). Hereditary Hearing Loss Homepage. World Wide Web URL: http://dnalab-www.uia.ac.be/dnalab/hhh.html
4. Steel, K.P. and Brown, S.D.M. (1994) *Trends Genet.* **10**, 428–435.
5. Nadeau, J.H., Kosowsky, M. and Steel, K.P. (1991) *Ann. N.Y. Acad. Sci.* **630**, 49–67.
6. Avraham, K.B., Hasson, T., Steel, K.P., Kingsley, D.M., Russell, L.B., Mooseker, M.S., Copeland, N.G. and Jenkins, N.A. (1995) *Nature Genet.* **11**, 369–375.
7. Gibson, F., Walsh, J., Mburu, P., Varela, A., Brown, K.A., Antonio, M., Beisel, K.W., Steel, K.P. and Brown, S.D.M. (1995) *Nature* **374**, 62–64.
8. Hasson, T. and Mooseker, M.S. (1996) *J. Biol. Chem.* **271**, 16431–16434.
9. Mooseker, M.S. and Cheney, R.E. (1995) *Annu. Rev. Cell Dev. Biol.* **11**, 633–675.
10. Weil, D., Blanchard, S., Kaplan, J., Guilford, P., Gibson, F., Walsh, J., Mburu, P., Varela, A., Levilliers, J., Weston, M.D., Kelley, P.M., Kimberling, W.J., Wagenaar, M., Levi-Acobas, F., Larget-Plet, D., Munnich, A., Steel, K.P., Brown, S.D.M. and Petit, C. (1995) *Nature* **374**, 60–61.
11. Hasson, T. and Mooseker, M.S. (1994) *J. Cell Biol.* **127**, 425–440.
12. Walker, J.E., Saraste, M., Runswick, M. J. and Gay, N.J. (1982) *EMBO J.* **1**, 945–951.
13. Lupas, A., VanDyke, M. and Stock, J. (1991) *Science* **252**, 1162–1164.
14. Kellerman, K.A. and Miller, K.G. (1992) *J. Cell Biol.* **119**, 823–834.
15. Mermall, V., McNally, J.G. and Miller, K.G. (1994) *Nature* **369**, 560–562.
16. Mermall, V. and Miller, K.G. (1995) *J. Cell Biol.* **129**, 1575–1588.
17. Dib, C., Fauré, S., Fizames, C., Samson, D., Drouot, N., Vignal, A., Millasseau, P., Marc, S., Hazan, J., Seboun, E., Lathrop, M., Gyapay, G., Morissette, J. and Weissenbach, J. (1996) *Nature* **380**, 152–154.
18. Brzeska, H., Lynch, T.J. and Korn, E.D. (1990) *J. Biol. Chem.* **265**, 3591–3594.
19. Bement, W.M. and Mooseker, M.S. (1995) *Cell Motil. Cytoskeleton* **31**, 87–92.
20. Bolker, J.A. and Raff, R.A. (1996) *BioEssays* **18**, 489–494.
21. Tilney, L.G., Cotanche, D.A. and Tilney M.S. (1992) *Development* **116**, 213–226.
22. Gillespie, P.G., Wagner, M.C. and Hudspeth, A.J. (1993) *Neuron* **11**, 581–594.
23. Hasson, T., Heintzelman, M.B., Santos-Sacchi, J., Corey, D.P. and Mooseker, M.S. (1995) *Proc. Natl. Acad. Sci. USA* **92**, 9815–9819.
24. Copeland, N.G., Jenkins, N.A., Gilbert, D.J., Eppig, J.T., Maltais, L.J., Miller, J.C., Dietrich, W.F., Weaver, A., Lincoln, S.E., Steen, R.G., Stein, L.D., Nadeau, J.H. and Lander, E.S. (1993) *Science* **262**, 57–66.
25. Nadeau, J.H. and Sankoff, D. (1997) *Nature Genet.* **15**, 6–7.
26. Hasson, T., Skowron, J.F., Gilbert, D.J., Avraham, K.B., Perry, W.L., Bement, W.M., Anderson, B.L., Sherr, E.H., Chen, Z.-Y., Greene, L.A., Ward, D.C., Corey, D.P., Mooseker, M.S., Copeland, N.G. and Jenkins, N.A. (1996) *Genomics* **36**, 431–439.
27. Board, P.G. and Webb, G.C. (1987) *Proc. Natl. Acad. Sci. USA* **84**, 2377–2381.
28. Jin, H., Oksenberg, D., Ashkenazi, A., Peroutka, S.J., Duncan, A.M., Rozmahel, R., Yang, Y., Mengod, G., Palacios, J.M. and O'Dowd, B.F. (1992) *J. Biol. Chem.* **267**, 5735–5738.
29. O'Neill, M.E., Marietta, J., Nishimura, D., Wayne, S., Van Camp, G., Van Laer, L., Negrini, C., Wilcox, E.R., Chen, A., Fukushima, K., Ni, L., Sheffield, V. and Smith, R.J.H. (1996) *Hum. Mol. Genet.* **5**, 853–856.
30. Chirgwin, J.M., Przybyla, A.E., MacDonald, R.J. and Rutter, W. (1979) *Biochemistry* **18**, 5294–5299.
31. Fan, Y.-S., Davis, L.M. and Shows, T.B. (1990) *Proc. Natl. Acad. Sci. USA* **87**, 6223–6227.
32. Bell, D.W., Taguchi, T., Jenkins, N.A., Gilbert, D.J., Copeland, N.G., Gilks, C.B., Zweidler-McKay, P., Grimes, H.L.,Tsichlis, P.N. and Testa, J.R. (1995) *Cytogenet. Cell Genet.* **70**, 263–267.
33. Devereux, J., Haeberli, P. and Smithies, O. (1984) *Nucleic Acids Res.* **12**, 387–395.